

## PREDICTING PERMEABILITY FROM NUCLEAR MAGNETIC RESONANCE AND ELECTRICAL PROPERTIES MEASUREMENTS

G. A. LaTorraca\*, K. J. Dunn\*, and R. J. S. Brown\*\*

\*Chevron Petroleum Technology Company  
P. O. Box 446, La Habra, CA 90633-0446

\*\*Chevron Annuitant

### ABSTRACT

Nuclear Magnetic Resonance (NMR) and electrical formation factor measurements are combined to yield predictions of permeability that are consistent with published results from researchers at Schlumberger and Univ. of Bologna/AGIP. For measurements on 7 clastic reservoirs, permeability is predicted within a factor of 3.2 and for a single reservoir this uncertainty is reduced to a factor of 2. For brine saturated samples, porosity is predicted to within 1.1 porosity units independent of lithology. For samples desaturated to nearly their "irreducible" values, brine saturation is determined with an uncertainty of 3.2 saturation units.

We assert that the measurement of the average  $T_1$  relaxation rate is accurate only when the distribution of  $T_1$  is adequately sampled. Under this condition, the average relaxation rate is proportional to the surface area. Consistent with this assertion, the product of the brine saturation and the average rate at that saturation is found to be equal to the average rate at full brine saturation for 5 well sorted chalk samples from a single field.

In our permeability calculations, we use the amplitude weighted geometric mean of the  $T_1$  distribution as the NMR parameter. We find the geometric mean to be essentially equivalent to the two parameter, stretched exponential representation in predicting permeability.

## INTRODUCTION

Nuclear Magnetic Resonance measurements have been used to estimate the permeability of rocks since 1966<sup>1</sup>. Additionally, NMR measurements<sup>1-8</sup> have been used to determine physical properties such as: porosity, water saturation, pore size distribution, pore surface to volume ratio, wetting phases, oil viscosity, diffusion, as well as image the distribution and flow of fluids through porous media.

A nuclear magnetism log<sup>9</sup> was initially designed by Chevron and Borg Warner and later developed into a commercial tool (NML) by Schlumberger. It was used for many years with variable success. Because of reliability issues, the need to dope the mud, signal to noise problems, high power requirements, and slow logging speed, the use of the tool has diminished with time. New tools such as NUMAR's MRIL (Magnetic Resonance Imaging Log) and Schlumberger's experimental PNMT (Pulsed Nuclear Magnetic Tool) appear to have solved all of the problems of the earlier tool (except for logging speed) and have caused renewed interest in NMR logging by the petroleum industry. With this renewed interest, our initial goal was to use a large Chevron dataset to evaluate existing algorithms and transforms for estimating permeability, porosity, and water saturation from NMR and electrical properties measurements.

## PERMEABILITY PREDICTION FOR CLASTICS

### A. Multiple Field Permeability Predictors

The longitudinal relaxation ( $M(t)$ ) of a brine saturated rock can be represented as a sum of exponentials<sup>5,10</sup>:

$$M(t) = \sum_{i=1}^n A_i e^{-t/T_{1i}} \quad (1)$$

Assuming fast diffusion<sup>11</sup>, the distribution of  $T_1$  values in equation (1) can be interpreted as a pore size distribution<sup>5</sup>. This interpretation is based on the assumption that similar pore sizes yield similar relaxation rates. The sum of exponentials is a useful representation for inferring pore size distributions but is difficult to incorporate in permeability prediction algorithms. Consequently, Kenyon et al.<sup>4</sup> introduced the stretched exponential representation of  $M(t)$  which is of the form:

$$M(t) = M_0 e^{-(t/T_{1\alpha})^\alpha} \quad (2)$$

where  $\alpha$  is the exponent which typically ranges between 0.5 and 0.7 (for their database) and  $T_{1\alpha}$  is the stretched exponential form of  $T_1$ . This representation allowed them to use a single, distribution weighted, relaxation time  $T_{1\alpha}$  in their algorithms for predicting

permeability. Using this representation, Kenyon et al.<sup>4</sup> found that for 60 samples, the best estimator of permeability was  $T_{1\alpha}^2 \phi^4$  where  $\phi$  is the porosity. Based on their grain consolidation model, Banavar and Schwartz<sup>12</sup> proposed the ratio  $T_{1\alpha}^2/F^2$  as a predictor of permeability. Sen et al.<sup>7</sup> added 40 measurements of  $T_{1\alpha}$  and electrical formation factor ( $F$ ) to the Kenyon et al. dataset and found that  $T_{1\alpha}^2/F^2$  was a slightly better predictor than  $T_{1\alpha}^2 \phi^4$ . Borgia et al.<sup>8</sup> proposed the use of  $T_{1\alpha}^2/F$  as a permeability predictor maintaining that  $1/F$  represents the transport properties while  $T_{1\alpha}^2$  represents the distance scale. They found, however, that the  $T_{1\alpha}^2 \phi^4$  predictor was slightly better at predicting the permeabilities of 37 clean sandstones. (Note: the predictor  $T_{1\alpha}^2/F^2$  for the Borgia et al. data was also slightly better than the  $T_{1\alpha}^2/F$  predictor.) The results of these analyses are summarized in Table 1.

The Schlumberger researchers<sup>4,5,7</sup> adopted the use of the stretched exponential representation to minimize the number of parameters used to predict permeability while retaining a weighting of all the data in  $M(t)$ . Brown and Fantazzini<sup>13</sup> introduced the geometric mean ( $T_{1G}$ ) of the component  $T_1$  values as an alternative, single parameter for predicting permeability. We chose to use the  $T_{1G}$  representation because we could readily calculate it from the  $T_1$  analysis available in the Chevron NMR datafiles. Additionally, the  $T_1$  distributions reported by Kenyon et al.<sup>5</sup> appear approximately log normal and, thus, well represented by the geometric mean. The Chevron NMR data, acquired between 1975 and 1983, are available in the form of a 6 component fit to the  $T_1$  relaxation curve with the bulk (brine) relaxation rate ( $1/T_{1b}$ ) removed, i.e.

$$M(t) = M_0(Ae^{-t/T_{1A}} + Be^{-t/T_{1B}} + Ce^{-t/T_{1C}}) \quad (3)$$

$$A + B + C = 1$$

The geometric mean  $T_{1G}$  is calculated from:

$$T_{1G} = \exp(A \ln T_{1A} + B \ln T_{1B} + C \ln T_{1C}). \quad (4)$$

Kenyon et al.<sup>4</sup> provide their analysis in the forms of both equations (2) and (3). Consequently, we were able to calculate the values of  $T_{1G}$  for their data and compare these calculations with their published values of  $T_{1\alpha}$ . We found  $T_{1G}$  and  $T_{1\alpha}$  to be linearly related with:

$$T_{1\alpha} = -8.9 + 1.37T_{1G} \quad (5)$$

in the range of  $11 \text{ ms} \leq T_{1G} \leq 414 \text{ ms}$  with a RMS error of 12 milli-seconds and  $r^2 = .993$ .

Thus, we expect our results using  $T_{1G}$  to be equivalent to those using  $T_{1\alpha}$ . Additionally, one of us (RJSB) contends that the calculation of  $T_{1\alpha}$  must be carefully made to avoid an overweighting of short  $T_1$  components. The linear relation between  $T_{1G}$  and  $T_{1\alpha}$  leads us to believe that Kenyon et al.<sup>4</sup> avoided this potential pitfall.

Using  $T_{1G}$  to represent the longitudinal relaxation data, we analyzed a Chevron dataset of 260 clastic samples to determine how well we could predict permeability from values of  $T_{1G}$ ,  $F$ , and  $\phi$  based on the parameter combinations (models) suggested by Kenyon et al.<sup>4</sup>, Sen et al.<sup>7</sup> and Borgia et al.<sup>8</sup>. The models and the statistics of the fitting process are listed in Table 2 and the data edits in Appendix A. Consistent with the results of Kenyon et al.<sup>4</sup>, there was little difference in how well each combination of parameters could predict the measured air ( $K_{air}$ ) and brine ( $K_{brine}$ ) permeabilities. The best permeability predictor (by a very small margin) was  $(T_{1G}/F)^2$  as suggested in Sen et al.<sup>7</sup> (1990). As depicted in Figure 1, this combination of parameters predicted  $K_{air}$  within a factor of 3.2 while the other models predicted  $K_{air}$  within a factor of 3.3. The brine permeability predictions were slightly worse (within factors of 3.4 to 3.7). (This is three times better than typically obtained for most field applications). We speculate that major contributors to the uncertainty in these predictions are: fine scale heterogeneity in the samples and differences in surface relaxation not only from reservoir to reservoir but also between reservoir facies.

## B. Single Field Permeability Predictors

We have shown that permeability can be predicted within a factor of 3.3 for clastic samples from 18 wells in 7 reservoirs. We believe this uncertainty can be reduced for an individual field where high quality data has been taken. An example of such an improvement is the clastic dataset depicted in Figures 2-4. This dataset contains electrical properties and NMR measurements on 57 samples from the spatially heterogeneous, delta top zone of an oil field. Because of the heterogeneity, the permeability range is large ( $0.5 \text{ md} < K_{air} < 5000 \text{ md}$ ). From X-ray diffraction measurements, almost all of the samples contain minimal to moderate (up to 20%) amounts of pore-filling kaolinite; a lesser number contain minor amounts of illite; and 12 samples contain minor amounts of pyrite (<5%), while 3 samples have more than 5% pyrite. The amount of clay had minor effects on the electrical properties of these samples but had a major effect on the permeability as can be seen by the correlations depicted in Figure 2 where brine permeability is cross-plotted with a measure of the clay content,  $Q_v$ , which is the CEC converted to units of milli-equivalents/pore volume.

As shown in Figures 3 and 4, both the air and brine permeabilities could be predicted from  $T_1$ ,  $F$ , and  $F^*$  (clay-corrected formation factor) measurements to within a factor of 2. This is a significant improvement over the fit to the combined clastic dataset (Fig.1). Such an improvement offers the possibility of developing accurate permeability algorithms for individual fields as needed. This is especially true in light of the extensive improvements that have been made in NMR technology since the early 1980s when our measurements were made.

## POROSITY FROM NMR $T_2$ MEASUREMENTS

The amplitude (A) of the NMR relaxation response has been described by Brown and

Gamson<sup>9</sup> as proportional to the number of protons sensed. This usually translates to the volume of brine in a brine saturated sample but can be extended to oil saturated rocks because liquid crude oils often have proton densities nearly the same as brine. (For gas saturated rocks, we would be getting an estimate of liquid saturation.) By comparing the amplitudes of the relaxation curves to similar measurements on porosity standards (Timur<sup>2,3</sup>), we can obtain estimates of porosity ( $\phi$ ) through:

$$\phi_{\text{sample}} = \phi_{\text{std}} \cdot A_{\text{sample}} / A_{\text{std}}. \quad (6)$$

Additional dimension corrections may also be required. The standards are made using a volume of brine and deuterium oxide ( $D_2O$ ). The  $D_2O$  produces no NMR response at the proton precession frequency. A 30% porosity standard, for example, contains 30% brine and 70%  $D_2O$ .

Figure 5 is a crossplot of porosity obtained gravimetrically by the Archimedes method (an industry standard) and porosity determined by NMR. The measurements were made on cores from 15 wells in 7 reservoirs. The samples are from both clastic and carbonate lithologies. For 278 points, the porosities determined by the Archimedes method could be predicted from the NMR determined porosities with a standard deviation of 1.07 porosity units (p.u.). We believe that these high accuracies support the assertion that NMR measurements can be used to accurately determine porosities independent of lithology. The data edits are described in Appendix A.

## BRINE SATURATION

As part of the electrical properties measurements, the brine saturations are determined from weights measured before and after desaturation against air using either the centrifuge or porous plate method. Alternatively, because the amplitudes of NMR relaxation curves are proportional to the number of protons in the brine, brine saturation can be determined from the ratio of the amplitudes (extrapolated to zero time) of the proton  $T_2$  (or  $T_1$ ) relaxation curves at partial and full brine saturation.

The brine saturations of 28 samples from 4 reservoirs were determined both from weights and NMR amplitude ratios. The results are depicted in Figure 6. The weight determined brine saturations were predicted from the NMR saturations within 3.2 saturation units. These data are consistent with the claim that brine saturation can be predicted from borehole measurements using properly calibrated NMR logging tools.

## RELAXATION RATE AND $S_w$

Few NMR studies on partially saturated rocks have been reported. Straley et al.<sup>14</sup> indicated that  $T_1$  distributions can be related to the amount and distribution of water removed by centrifuging. Halperin et al.<sup>15</sup> studied the surface relaxation rates for both  $T_1$  and  $T_2$  as a function of water saturation.

We suggest the use of the average relaxation rate to analyze partially desaturated rocks. From Eq.(1), the average relaxation rate can be expressed as:

$$\left\langle \frac{1}{T_1} \right\rangle = \frac{d \ln M(t)}{dt} \Big|_{t=0} = \sum \frac{A_i}{T_{1i}} \quad (7)$$

where, in the fast diffusion regime,  $1/T_{1i}$  can be approximated by:

$$\frac{1}{T_{1i}} \approx \frac{1}{T_{1b}} + \frac{\lambda}{T_{1s}} \frac{S_i}{V_i} \quad (8)$$

and  $T_{1b}$  and  $T_{1s}$  are respectively the bulk and surface relaxation time,  $S_i$  and  $V_i$ , the surface area and volume of the  $i$ -th pore, and  $\lambda$  the thickness of the surface layer. The summation is over all pores. Because the average relaxation rate is the logarithmic decrement of  $M(t)$  at  $t=0$  (Eq.(7)), the data collected at short times must be adequately sampled and be of high quality.

For a fully saturated rock, the average relaxation rate (with the bulk relaxation rate subtracted) can be written as:

$$\left\langle \frac{1}{T_1} \right\rangle = \sum A_i \frac{\lambda}{T_{1s}} \frac{S_i}{V_i} = \rho \sum \frac{V_i}{V_p} \frac{S_i}{V_i} = \frac{\rho S}{V_p} \quad (9)$$

where we assume the surface relaxation strength  $\rho$  ( $\equiv \lambda/T_{1s}$ ) is a constant and use the fact that  $A_i=V_i/V_p$ .  $V_p$  and  $S$  are respectively the total pore volume and surface of a porous rock sample.

When the rock is partially desaturated, we assume that the pore surfaces are always coated with enough water that a meaningful relaxation time measurement is possible. This assumption is supported by the experimental work of Halperin et al.<sup>15</sup> Consequently,  $S_i$  will be constant during the desaturation process, and the product of the saturation  $S_w$  and the averaged relaxation time  $\langle 1/T_{1,S_w} \rangle$  becomes:

$$S_w \cdot \left\langle \frac{1}{T_{1,S_w}} \right\rangle = S_w \cdot \rho \sum A_i \frac{S_i}{V_{i,S_w}} = S_w \cdot \rho \sum \frac{V_{i,S_w}}{V_{p,S_w}} \frac{S_i}{V_{i,S_w}} = \frac{\rho S}{V_p} \quad (10)$$

Thus, if  $S_i$  is constant during desaturation, the product of  $S_w \cdot \langle 1/T_{1,S_w} \rangle$  is a constant equal to  $\langle 1/T_1 \rangle$ . For a single sample at different desaturation stages,  $S_w \cdot \langle 1/T_{1,S_w} \rangle$  versus  $S_w$  should be a horizontal line. When applied to a set of rock samples,  $S_w \cdot \langle 1/T_{1,S_w} \rangle$  versus  $\langle 1/T_1 \rangle$  should be a straight line of slope one. In Figure 7, the product  $S_w \cdot \langle 1/T_{1,S_w} \rangle$  is plotted against  $\langle 1/T_1 \rangle$  for 5 chalk samples from a single field. As expected, the slope is nearly equal to one.

These chalks, however, have a narrow range of pore sizes and, consequently, a narrow range of  $T_{1i}$  components. In general, rocks have a wide distribution of pore sizes, including those which correspond to very small  $T_{1i}$ . Because the average relaxation rate is very sensitive to these small  $T_{1i}$  components, very accurate measurements near  $t=0$  are required. Unfortunately, much of our data is inadequately sampled near  $t=0$  for accurate average relaxation rate determinations.

## AREAS FOR FURTHER STUDY

We foresee the need for an improved understanding of transverse relaxation ( $T_2$ ) and restricted diffusion measurements for efficient use of new NMR logging tools. The early efforts in the oil industry were to use  $T_1$  data to estimate permeability. However, in logging,  $T_1$  measurements require the tool to be stationary for tens of seconds.  $T_2$  measurements can be made while the tool is being moved. Consequently, recent emphasis<sup>16</sup> has been on the use of  $T_2$  measurements to predict permeability as well as estimate porosity and saturation. There are significant difficulties in the measurement of  $T_2$  relaxation curves which appear to have been resolved by the NMR tool designers at NUMAR and Schlumberger. For example,  $T_2$  relaxations tend to be shorter than  $T_1$  relaxations. Thus, short delay times and fast digitizers are needed. Second,  $T_2$  measurements are complicated by fluid diffusion. The effects of fluid diffusion are minimized in the new tools by proper choices of Larmor frequency and pulse trains. Additionally, the new tools offer the possibility of measurements of diffusion which can be used to improve our ability to estimate permeability<sup>17</sup>.

## ACKNOWLEDGEMENTS

We thank Pat Worthington, Turk Timur, Del SeEVERS, and all the technicians (John Borely, Glen Porter, Mike Carlo, Jim Leather, Connie Hall, Rod Miller, Derrick Woo, Sam Bell, Dick Reynolds and others) involved in making the laboratory measurements documented in this paper. We also thank Barry Reik and Carol Meyer for the critical review of the manuscript.

## REFERENCES

1. Seevers, D. O.: "A Nuclear Magnetic Method for Determining the Permeability of Sandstones," *Trans.*, SPWLA (1966) Paper L.
2. Timur, A.: "Producible Porosity and Permeability of Sandstones Investigated Through Nuclear Magnetic Resonance Principles," *The Log Analyst* (Jan.-Feb. 1969) 3-11.
3. Timur, A.: "Pulsed Nuclear Magnetic Resonance Studies of Porosity, Moveable Fluid, and Permeability of Sandstones," *JPT* (1969) 775-86; *Trans.*, AIME, **246**.
4. Kenyon, W. E., Day, P. I., Straley, C., and Willemson, J. F.: "A Three-Part Study of NMR Longitudinal Relaxation Properties of Water-Saturated Sandstones," *SPE Formation Evaluation*, (Sept. 1988) 622-36.
5. Kenyon, W. E., Howard, J. J., Sezginer, A., Straley, C., Matteson, A., Horkowitz, K., and Ehrlich, R.: "Pore-size Distribution and NMR in Microporous Cherty Sandstones," *Trans.*, 30th Annual SPWLA Symposium (June 1989) Paper LL.
7. Sen, P. N., Straley, C., Kenyon, W. E., and Whittingham, M. S.: "Surface-to-Volume Ratio, Charge Density, Nuclear Magnetic Relaxation, and Permeability in Clay-Bearing Sandstones," *Geophysics* (1990) **55**, 61.
8. Borgia, G. C., Brighenti, G., Fantazzini, P., Fanti, G. D., and Mesini, E.: "Specific Surface and Fluid Transport in Sandstones Through NMR Studies," *SPE Formation Evaluation* (Sept. 1992), 206-10.
9. Brown, R. J. S. and Gamson, B. W.: "Nuclear Magnetism Logging," *JPT* (Aug. 1960) 199-201; *Trans.*, AIME, **219**.
10. Gallegos, D. P. and Smith, D. M.: "A NMR Technique for the Analysis of Pore Structure: Determination of Continuous Pore Size Distributions," *J. Coll. Interf. Sci.* **122** (Mar. 1988), 143-153.
11. Brownstein, K. R. and Tarr, C. E.: "Importance of Classical Diffusion in NMR Studies of Water in Biological Cells," *Phys. Rev. A.* (June 1979) **19**, 2446-53.
12. Banavar, J. R. and Schwartz, L. M.: " Probing Porous Media with Nuclear Magnetic Resonance," In J. Klafter and J. M. Drake (Editors), *Molecular Dynamics in Restricted Geometries*, chapter 10, J. Wiley, New York, N.Y. (1989).
13. Brown, R. J. S. and Fantazzini: "Conditions for Initial Quasi-linear  $T_2^{-1}$  vs.  $\tau$  for CPMG NMR with Diffusion and Susceptibility Differences in Porous Media and Tissues," Submitted to Physical Review B (Nov. 1992).
14. Straley, C., Morriss, C. E., Kenyon, W. E., and Howard, J. J.: "NMR in Partially Saturated Rocks: Laboratory Insights on Free Fluid Index and Comparison with Borehole Logs," *Trans.*, 32nd Annual SPWLA Symposium (June 1991) Paper CC.
15. Halperin, W. P., Bhattacharja, S., and D'Orazio, F.: "Relaxation and Dynamical Prop-



erties of Water in Partially Filled Porous Materials Using NMR Techniques," *Magnetic Resonance Imaging* 9, (1991), 733-7.

16. Jerosch-Herold, M., Thomann, H., Thompson, A. H.: "Nuclear Magnetic Resonance Relaxation in Porous Media," *Trans.*, 66th Annual Conference and Exhibition of the SPE Oct. 1991 Paper SPE 22861.
17. Kleinberg, R. L. and Horsfield, M. A.: "Transverse Relaxation Processes in Porous Sedimentary Rock," *J. of Magnetic Resonance* 88, (Sept. 1990), 9-19.

## APPENDIX A

### Measurement Procedures

The samples, typically 1" in diameter and 1.5" long, were solvent cleaned to a water wet state and saturated with brines comparable to their respective reservoir brines. Desaturation against air was done using a cooled centrifuge. Porosities and brine saturations were determined gravimetrically. The formation factors and brine permeabilities were measured at a confining pressure of 200 psi. Air permeability was determined from nitrogen gas flow with the sample subjected to 100-200 psi (usually 200 psi). The NMR measurements were all made on a Varian V-4012A magnet at a Larmor frequency of 10 MHz. The longitudinal relaxations were determined at 20 points (typically) using an inversion recovery pulse sequence.

### Data Edits

For permeability estimation: one complete set of measurements was removed because the brine  $T_1$  measurement was inexplicably low (0.622 seconds); 5 data points reported as questionable were removed; 5 shale samples, 26 vertical samples, and all carbonate samples were not included.

For porosity estimation: 4 data points were removed because three independent porosity determinations differed by more than 4 porosity units, and one data point was removed because the sample was extremely compressible and contained large chunks of fossilized wood. For brine saturation, 3 data points were removed because of the large uncertainty reported in the gravimetric determination of their saturations.

Table 1: Least-squares estimators for permeability from previous work

Reference	Permeability model*	$\sigma_k^\dagger$
Kenyon et al. (Ref. 4)	$K_{brine} = 1.17(T_{1\alpha}^2\phi^4)^{1.13}$	2.7
Sen et al. (Ref. 7)	$K_{brine} = 0.794(T_{1\alpha}/F)^{2.15}$	3.3
Borgia et al. (Ref. 8)	$K_{air} = 3.25(T_{1\alpha}^2/F^2)^{0.79}$	2.1
	$K_{air} = 0.076(T_{1\alpha}/F)^{0.94}$	2.3
	$K_{air} = 10.7(T_{1\alpha}^2\phi^4)^{0.72}$	1.9

\*The estimated permeability in md.  $T_{1\alpha}$  is in ms,  $\phi$  in fractions.

† $\sigma_k$  is the factor by which the estimated permeability misses the measured permeability. It is equal to  $10^{(\text{std err})}$  obtained from  $\log k = a + b \log(\text{predictor}) \pm (\text{std err})$ .

Table 2: Least-squares estimators for permeability from present work

$K_{air}(\text{md})$	$\sigma_k^\dagger$	$n^*$	$K_{brine}(\text{md})$	$\sigma_k^\dagger$	$n^*$
<u>All samples w/edits</u>					
$0.067(T_{1G}^2/F)^{1.02}$	3.3	260	$0.0063(T_{1G}^2/F)^{1.23}$	3.7	257
$2.25(T_{1G}/F)^{1.77}$	3.2	260	$0.43(T_{1G}/F)^{2.16}$	3.4	257
$1.85(T_{1\alpha}/F)^{1.67\dagger}$	3.2	260	$0.33(T_{1\alpha}/F)^{2.05\dagger}$	3.4	257
$5.31(T_{1G}^2\phi^4)^{.819}$	3.3	260	$1.21(T_{1G}^2\phi^4)^{1.00}$	3.6	257
$14.0(\sum_{i=1}^3 (A_i\phi)^4 T_{1i}^2)^{.763}$	3.3	260	$4.00(\sum_{i=1}^3 (A_i\phi)^4 T_{1i}^2)^{.933}$	3.7	257
<u>Clastic Subset</u>					
$0.89(T_{1G}/F)^{1.90}$	1.96	57	$0.29(T_{1G}/F)^{2.16}$	2.00	57
$1.32(T_{1G}/F^*)^{1.81}$	1.96	57	$0.45(T_{1G}/F^*)^{2.06}$	1.99	57

† $\sigma_k$  is the factor by which the estimated permeability misses the measured permeability. It is equal to  $10^{(\text{std err})}$  obtained from  $\log k = a + b \log(\text{predictor}) \pm (\text{std err})$ .

‡ $T_{1\alpha}$  was obtained using Eq.(5).

\*Number of samples.

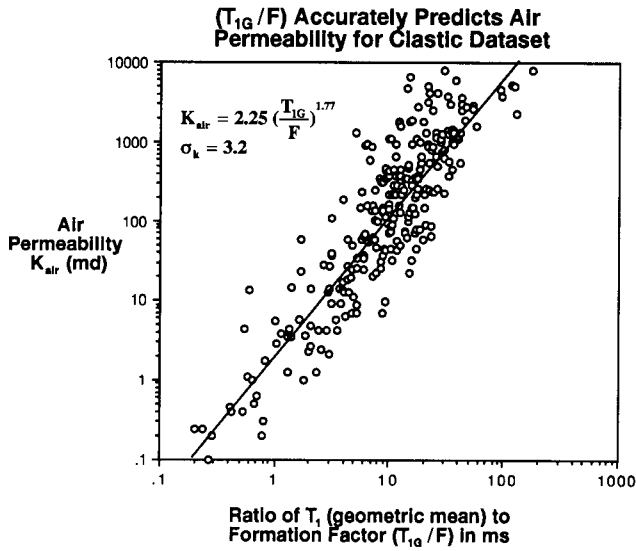


Figure 1

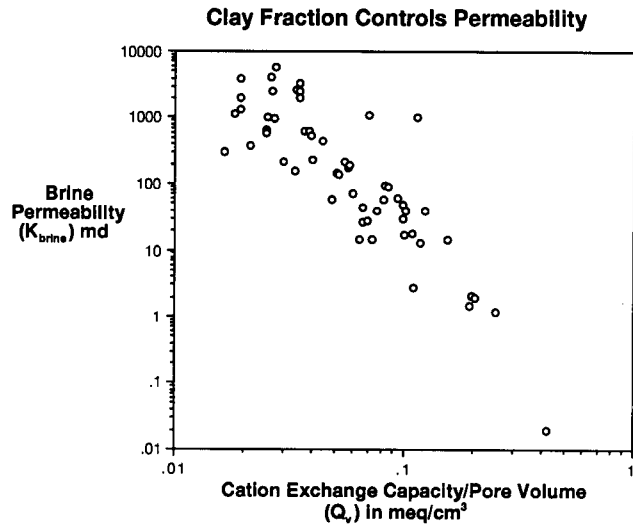


Figure 2

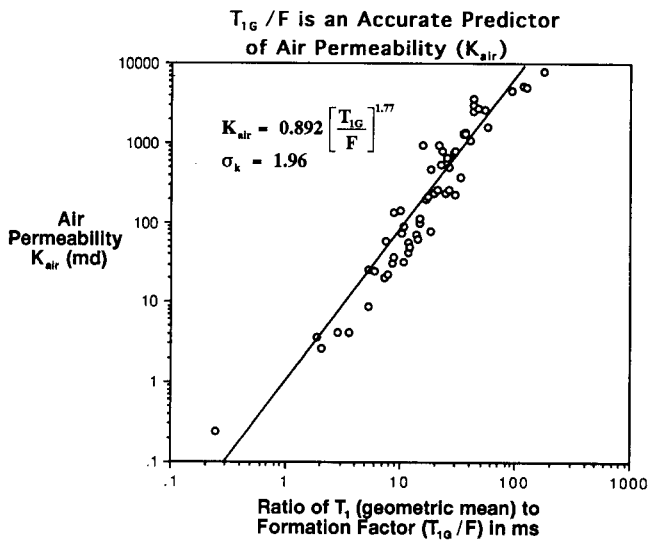


Figure 3a

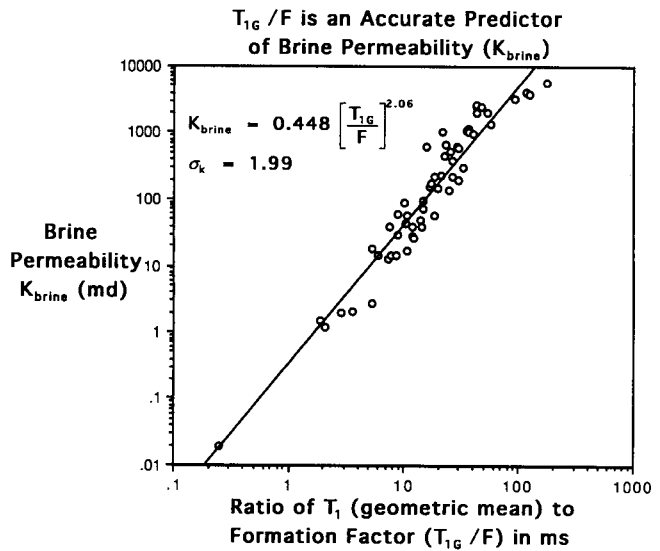


Figure 3b

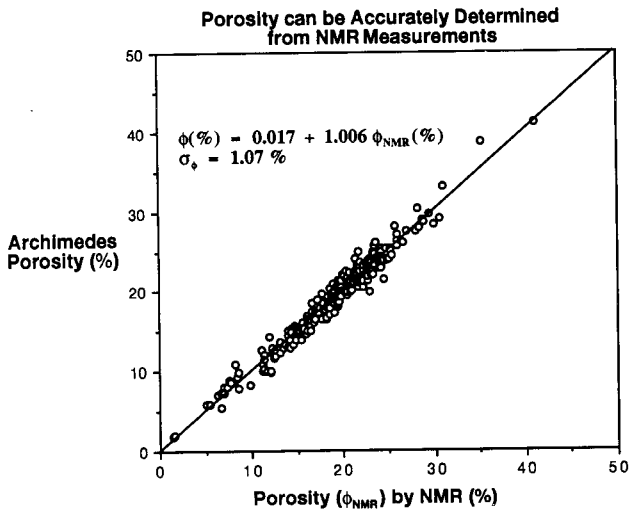


Figure 4

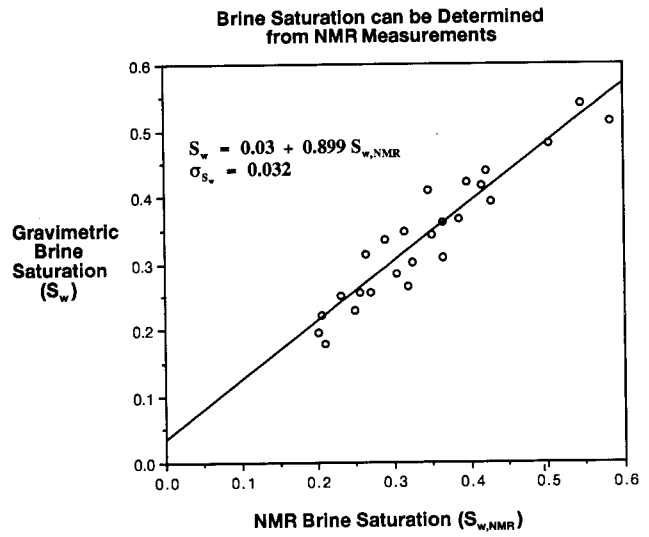


Figure 5

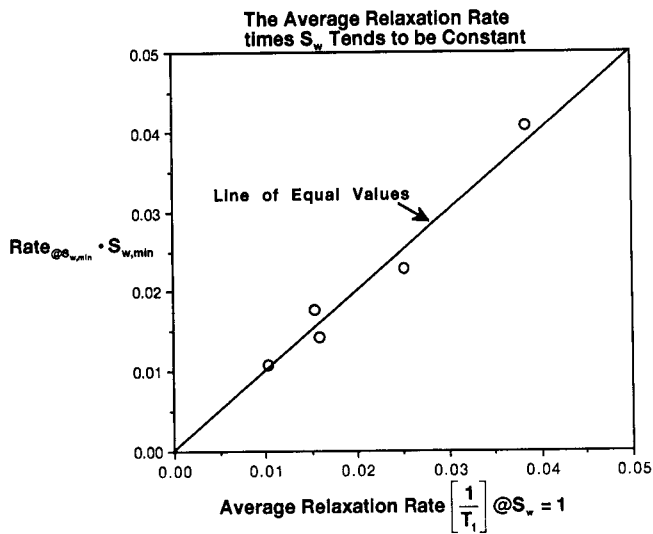


Figure 6